Comparison of the Phase Behavior of Some Selected Binary Systems with Ionic Liquids

Alireza Shariati, Karin Gutkowski, and Cor J. Peters
Physical Chemistry and Molecular Thermodynamics, DelftChemTech, Faculty of Applied Sciences, Delft University of Technology, Delft, The Netherlands

DOI 10.1002/aic.10384
Published online March 15, 2005 in Wiley InterScience (www.interscience.wiley.com).

The phase behavior of binary mixtures consisting of two different supercritical fluids, one with no dipole moment and the other one with a strong dipole moment, and an imidazolium-based ionic liquid were studied experimentally. Carbon dioxide (CO_2) and trifluoromethane (CHF_3), and 1-butyl-3-methylimidazolium hexafluorophosphate ([bmim][PF_6]) were the selected supercritical fluids and ionic liquid, respectively. A synthetic method was used to measure liquid–vapor (LV) and liquid–liquid–vapor (LLV) boundaries of these binary systems. Results for the LV boundaries are reported for CO_2 concentrations ranging from 10.0 to 65.0 mol % and within temperature and pressure ranges of 293.29–363.54 K and 0.59–73.50 MPa, and for CHF_3 concentrations ranging from 10.2 to 99.0 mol % and within temperature and pressure ranges of 303.20–363.42 K and 0.58–41.00 MPa, respectively. The LV boundaries of pure CO_2 and CHF_3 were measured up to their critical points. For the binary systems consisting of either CO_2 or CHF_3 with [bmim][PF_6], the LLV boundaries were similarly measured up to their critical endpoints. The experimental results obtained in this work show that the binary systems of CO_2 or CHF_3 + [bmim][PF_6] have Type III phase behavior according to the classification of Scott and Van Konynenburg. To the extent available, the experimental data obtained for the system CO_2 + [bmim][PF_6] were compared with literature data. In addition, comparisons were made with literature data of binary systems of either CO_2 or CHF_3 with other ionic liquids belonging to the same homologous family. *AIChE J,* 51: 1532–1540, 2005
Keywords: 1-butyl-3-methylimidazolium hexafluorophosphate, carbon dioxide, trifluoromethane; phase behavior, binary systems, ionic liquid, experimental

Introduction

Conventional organic solvents are widely used in chemical processes, such as in reactions and separations. However, because these solvents strongly affect the quality of life as a consequence of losses into the environment, there is a strong driving force to replace them by less hazardous ones. Because they are volatile, they are easily emitted into the atmosphere, and because they are used in substantial quantities, their danger is realistic and serious. In addition, because of their flammability, serious problems may arise in handling traditional organic solvents.

Ionic liquids (ILs) are organic salts consisting of anions and cations. Almost all of them have melting points below 100°C, the majority of which are in the liquid phase at room temperature. The most commonly used cations in ILs are imidazolium, pyrrolidinium, and pyrrodonium, whereas the most popular anions consist of chloride, nitrate, acetate, hexafluorophosphate, and tetrafluoroborate. In addition, an alkyl chain may be attached to the cation of an IL. Variations in any of the above-mentioned segments of the IL molecule provide numerous options to modify and control the physical and chemical

Correspondence concerning this article should be addressed to C. J. Peters at Cor.Peters@tnw.tudelft.nl.

properties of the ILs. For example, whereas 1-alkyl-3-methyl imidazolium hexafluorophosphate ILs are immiscible with water, 1-alkyl-3-methylimidazolium nitrate ILs are completely miscible with water.[1] Similarly, the hydrophobicity of an IL increases with increasing chain length of the alkyl chain.[2] Therefore, ILs can be designed to meet a particular application. From the flexibility in combining anions and cations, along with the many possibilities to vary all kind of functional groups, it becomes apparent that the number of possible ILs will be almost unlimited.

Based on the unique characteristics of ILs, they are considered as the next generation of solvents having the potential to replace conventional organic solvents. ILs do not possess significant vapor pressures and thus do not pollute the atmosphere. For the same reason, they reduce the working exposure hazards because inhalation by the respiratory system is not possible. On the other hand, they have amazingly good solvent power for both organic and inorganic materials. They are nonflammable and thermally stable and most of them are stable in air and water. They usually have favorable densities and viscosities. Recently, Brennecke and Maginn[3] gave a comprehensive perspective about the potential applications of ILs in catalytic reactions, gas separations, liquid separations, cleaning operations, electrolyte/fuel cells, and as lubricants and heat transfer fluids.

Until now, many articles have been published on synthesizing ILs[4-9] or the applications of ILs in catalytic reactions as solvents.[10-17] There are also a number of papers suggesting liquid–liquid separations using ILs.[18-23] Recently, Brennecke and coworkers presented two possible applications for ILs using supercritical fluids.[24-26] One application is the recovery of certain organic products from ILs using supercritical CO_2.[24] The main advantage of this process is the lack of cross-contamination between the IL and supercritical CO_2. Another application proposed by Scurto et al.[25] is the use of supercritical CO_2 for separating ILs from organic solvents. Application of supercritical CO_2 induces the formation of an additional liquid phase that is rich in IL, even when the original solution is quite dilute in IL. In other words, the extraction of organic materials can be achieved without any IL contamination in the final recovered product. Later, Scurto et al.[26] showed that the introduction of CO_2 can even allow separation of both hydrophobic and hydrophilic imidazolium-based ILs from aqueous solutions. For example, 1-butyl-3-methylimidazolium hexafluorophosphate ([bmim][PF_6]) can be separated from an IL-saturated aqueous solution at 293 K and at a CO_2 pressure of 4.9 MPa.

Literature focusing on describing the phase behavior of the systems of ILs + supercritical fluids are extremely scarce. Such studies constitute an absolute prerequisite for a better understanding and designing of processes involving both ILs and supercritical fluids. For that purpose, the major objective of the work described in this article was to gain more insight into the phase behavior of supercritical fluid + IL systems; more specifically, we set out to investigate experimentally the binary systems CO_2 + [bmim][PF_6] and CHF_3 + [bmim][PF_6]. Solubilities of CO_2 in [bmim][PF_6], CHF_3 in [bmim][PF_6], and [bmim][PF_6] in CHF_3 were measured. The liquid–vapor (LV) saturated vapor pressure curves of pure CO_2 and CHF_3 were determined up to their critical points. In addition, the liquid–liquid–vapor (LLV) three-phase equilibria in the systems CO_2 + [bmim][PF_6] and CHF_3 + [bmim][PF_6] up to their critical endpoints were determined as well. The phase behavior results of these systems were related to the fluid-phase behavior classification of Scott and Van Konynenburg.[27]

Results of the system CO_2 + [bmim][PF_6] were compared to similar data of Brennecke and coworkers,[28-30] Maurer and coworkers,[31] and Han and coworkers,[32] who also studied this system in recent years.

Experimental

High-pressure experiments were carried out in an autoclave for the higher concentrations of CO_2 and CHF_3 ($x_{CO2} > 0.399$ and $x_{CHF3} > 0.483$). The Cailletet apparatus was used at lower concentrations of CO_2 and CHF_3 ($x_{CO2} \leq 0.399$ and $x_{CHF3} \leq 0.483$), where equilibrium pressures were not so high. Both facilities operate according to the synthetic method, where phase transitions are visually observed for a sample of fixed overall concentration at varying temperatures and pressures.

The temperature measurement of the Cailletet apparatus has an accuracy of ± 0.01 K. In the Cailletet apparatus, the pressure is kept constant and measured with a dead weight gauge with an uncertainty of ± 0.01 MPa. On the other hand, the accuracy of the pressure measurements in the autoclave apparatus is better than $\pm 0.04\%$ of the pressure reading (from 3.0 to 100.0 MPa), whereas the uncertainty in the measured bubble point temperatures is ± 0.051 K. The uncertainty in determining the critical point and the critical endpoint temperatures is ± 0.08 K. Details of the experimental facilities and procedures can be found elsewhere.[33]

The CO_2 used for the measurements was supplied by Messer Griesheim and had an ultra-high purity of 99.995%. The CHF_3 was obtained form Paraxair and was ultra pure (purity: 99.995%). The liquid [bmim][PF_6], used for the CO_2 + [bmim][PF_6] measurements, was purchased from Fluka. However, [bmim][PF_6] used in the CHF_3 + [bmim][PF_6] experiments was kindly provided by Prof. Seddon of the Queen's University of Belfast, Northern Ireland. In both binary systems, the [bmim][PF_6] was dried under vacuum at room temperature for several days before use. Water content of the dried IL, determined by Karl–Fischer analysis, was always <0.02 wt%.

Results and Discussion

The system CO_2 + [bmim][PF_6]

The solubility of CO_2 in [bmim][PF_6] was determined by measuring the bubble point pressures of the binary system CO_2 + [bmim][PF_6] at different temperatures for several isopleths. Table 1 summarizes the experimental results of this system. By analyzing these data, it is evident that with increasing CO_2 concentration, the sensitivity of the equilibrium pressure (P) to temperature (T) increases because the P–T slopes become steeper (slopes of about 0.02 MPa/K for the line at $x_{CO2} = 0.10$ and of 0.52 MPa/K for the line at $x_{CO2} = 0.65$). It can also be seen that at lower concentrations of CO_2, the equilibrium pressure of the system is very low. However, when the CO_2 concentration further increases isothermally, the equilibrium pressures increase dramatically. This can be more easily observed on a P–x diagram obtained by interpolating the experimental data of Table 1. To obtain the P–x diagram of this system at constant temperature, a second-order polynomial was

Table 1. Vapor–Liquid Equilibrium Data for Various Concentrations (in mole fraction) of Carbon Dioxide in the CO_2 + [bmim][PF_6] System

x_{CO2}	T (K)	P (MPa)	T (K)	P (MPa)	T (K)	P (MPa)
0.100	298.29	0.59	323.45	0.93	348.38	1.34
	303.35	0.65	328.43	1.01	353.25	1.43
	308.31	0.71	333.39	1.09	358.16	1.53
	313.35	0.78	338.66	1.17	363.45	1.63
	318.35	0.85	343.51	1.26		
0.203	303.21	1.45	328.23	2.24	353.24	3.25
	308.23	1.58	333.25	2.43	358.17	3.45
	313.27	1.74	338.13	2.61	363.27	3.69
	318.24	1.91	343.29	2.83		
	323.19	2.08	348.20	3.07		
0.250	293.32	1.53	318.62	2.50	343.48	3.79
	298.32	1.69	323.39	2.77	348.59	4.05
	303.33	1.88	328.41	2.97	353.31	4.31
	308.34	2.07	333.46	3.25	358.44	4.61
	313.35	2.29	338.59	3.49	363.28	4.93
0.351	293.29	2.43	318.35	4.09	343.39	6.22
	298.28	2.73	323.31	4.47	348.41	6.72
	303.29	3.09	328.28	4.85	353.50	7.22
	308.33	3.37	333.39	5.29	358.40	7.70
	313.32	3.71	338.32	5.76	363.46	8.24
0.399	293.56	2.97	318.31	5.01	343.46	7.73
	298.52	3.29	323.35	5.47	348.44	8.37
	303.28	3.69	328.31	6.01	353.42	9.05
	308.23	4.13	333.38	6.55	358.35	9.67
	313.21	4.51	338.47	7.15	363.54	10.43
0.501	312.97	6.88	327.99	9.72	342.90	13.46
	318.02	7.72	332.73	10.84	347.58	14.80
	323.00	8.68	337.82	12.10	352.81	16.30
0.598	313.00	25.36	327.94	31.70	342.82	39.60
	317.99	26.74	332.67	34.50	347.57	42.18
	322.96	29.20	337.81	37.10	352.53	43.90
0.650	313.03	52.66	327.91	61.36	342.52	68.78
	318.03	55.60	332.87	63.90	347.49	71.14
	322.99	58.62	337.79	66.30	352.60	73.50

fit to each isopleth of the P–T diagram. Figure 1 shows the phase behavior of the system CO_2 + [bmim][PF_6] in such a P–x diagram at 330, 340, and 350 K. As expected, with increasing temperature at fixed pressure, the solubility of CO_2 in the IL phase decreases. Every isotherm of Figure 1 indicates the high solubility of CO_2 in [bmim][PF_6] at low pressures. However, any further increase of the CO_2 concentration requires rapidly increasing pressures, which is a quite significant behavior of the ILs investigated. Normally, when a large amount of CO_2 dissolves in a liquid phase at low pressures, the system shows a "simple" phase envelope with a mixture critical point at moderate pressures.

Recently, Shariati and Peters[34,35] measured the phase behavior of the binary systems CO_2 + 1-ethyl-3-methylimidazolium hexafluorophosphate ([emim][PF_6]) and CO_2 + 1-hexyl-3-methylimidazolium hexafluorophosphate ([hmim][PF_6]). Figure 2 compares the phase diagrams of these two binary systems with the system CO_2 + [bmim][PF_6] at 333.15 K. The measurements show the similarities in phase behavior of the three binary CO_2 systems with [emim][PF_6], [bmim][PF_6], and [hmim][PF_6], respectively. In all three of these binary systems, CO_2 shows very high solubilities in each IL at lower pressures, whereas the equilibrium pressures increase steeply at higher compositions of CO_2. In addition, it is seen that, although the solubilities of CO_2 in the three different 1-alkyl-3-methylimidazolium hexafluorophosphates almost coincide for an isotherm at lower pressures, they differ substantially at elevated pressures. It is clear from Figure 2 that the solubility of CO_2 in ILs at fixed temperature and pressure increases by increasing the alkyl chain length.

Brennecke and coworkers measured the phase behavior of CO_2 + [bmim][PF_6] in three different studies.[28-30] They experimentally determined the phase behavior of this system for the first time in 1999.[28] Later, however, they noticed that because the [bmim][PF_6] used in their previous study was saturated with water, the experimental solubility data of CO_2 in [bmim][PF6] had been dramatically affected by the presence of great quantities of water.[29] It was reported that at 295.15 K, the water content of [bmim][PF_6] was as high as 2.3 wt %. There-

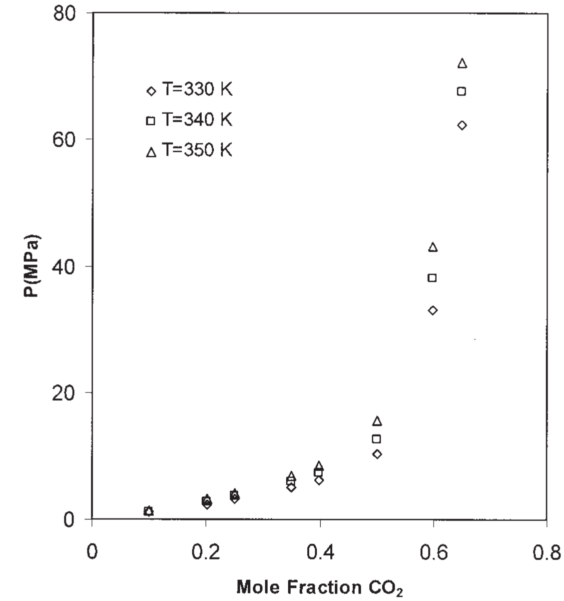

Figure 1. P–x diagrams of the system CO_2 + [bmim][PF_6] at 330, 340, and 350 K.

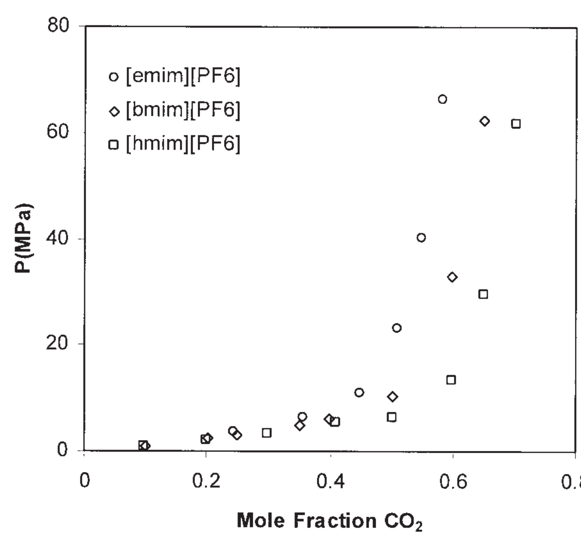

Figure 2. P–x diagrams of the binary systems CO_2 + [emim][PF_6], CO_2 + [bmim][PF_6], and CO_2 + [hmim][PF_6] at 333.15 K.

fore, in a next study, the purity of the liquid [bmim][PF_6] was increased before use by drying under vacuum at room temperature for several days, resulting in a water content in [bmim][PF_6] of about 0.15 wt %, as measured by a Karl–Fischer analysis. They compared the phase behavior of the binary CO_2 systems with both undried and dried samples at 313.15 K. Blanchard et al.[29] reported that the difference in CO_2 solubility of both samples at 5.7 MPa, for instance, was dramatic: 0.54 in the mole fraction of CO_2 for the dried [bmim][PF_6] compared to only 0.13 in the mole fraction for the water-saturated [bmim][PF_6]. In addition, Anthony et al.[30] measured the solubility of CO_2 in [bmim][PF_6] at lower pressures (<1.4 MPa) using a more accurate experimental method. They noticed that the solubility of CO_2 in [bmim][PF_6] was only in qualitative agreement with previously published results by Blanchard et al.[29] According to the trend in their measurements, it is clear that the solubility of CO_2 in [bmim][PF_6] cannot be as high as that reported by Blanchard et al. in 2001. Figure 3 compares the results of this work for the solubility of CO_2 in [bmim][PF_6] with those of both Blanchard et al.[29] and Anthony et al.[30] at 323.15 K, showing very good agreement with the latter. Anthony et al.[30] calculated Henry's constants for CO_2 in [bmim][PF_6] using the limiting slope in the *P–x* diagram (Henry's constant line), that is, with CO_2 solubility approaching zero. They reported Henry's constants of CO_2 in [bmim][PF_6] to be 3.87 ± 0.04, 5.34 ± 0.03, and 8.13 ± 0.05 MPa at 283.15, 298.15, and 323.15 K, respectively. The Henry's constant line at 323.15 K, as depicted in Figure 3, further confirms the good agreement between the results of this work and those of Anthony et al.[30]

In addition to this work, Blanchard et al.,[29] Perez-Salado Kamps et al.,[31] and Liu et al.[32] also reported the solubility of CO_2 in [bmim][PF_6] at a temperature of 333.15 K. Figure 4 shows a comparison of all these experimental data, indicating excellent agreement between our results and those of Perez-Salado Kamps et al., especially by considering that the experimental facilities and methods used were completely different.

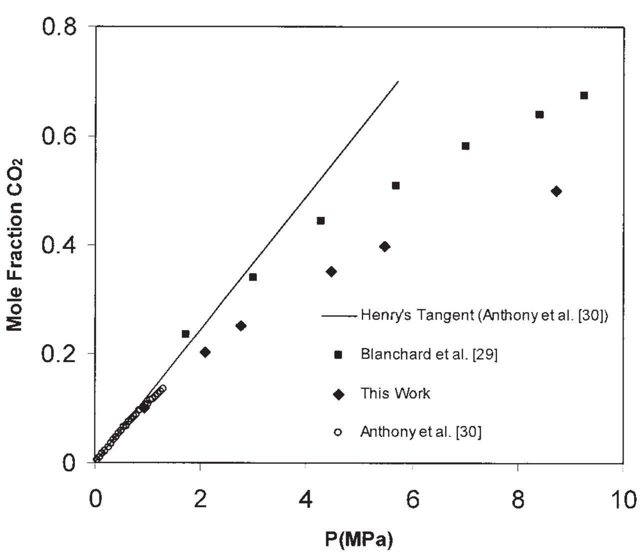

Figure 3. Comparison between the results of this work and literature data on the system CO_2 + [bmim][PF_6] at 323.15 K.

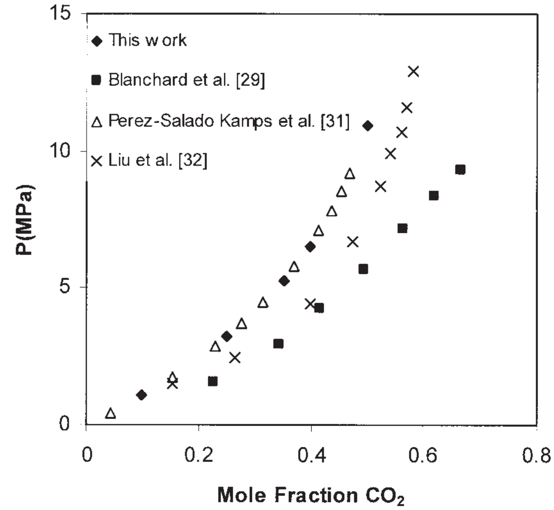

Figure 4. Comparison between the results of this work and literature data on the system CO_2 + [bmim][PF_6] at 333.15 K.

The data of Blanchard et al.[29] and Liu et al.[32] show greater deviations from our data, which become even more significant with increasing pressure at constant temperature.

To be able to determine the type of fluid phase behavior of the system CO_2 + [bmim][PF_6], the occurrence of the second liquid phase was also investigated in a temperature and pressure range close to the critical point of the more volatile component (CO_2). For that purpose, a mixture of 98.0 mol % CO_2 and 2.0 mol % [bmim][PF_6] was prepared and its phase behavior was studied experimentally. Within the uncertainty of the experimental data, in this system a three-phase locus L_1L_2V was found, which turned out to be almost undistinguishable compared to the location of the LV line of pure CO_2. In addition, a critical endpoint of the nature (L_1 = V) + L_2 was found in the system CO_2 + [bmim][PF_6], that is, in this point the L_1 and V phases are critical in the presence of L_2. This critical endpoint also is almost undistinguishable from the critical point of pure CO_2. According to the classification of fluid-phase behavior of Scott and Van Konynenburg, this system could have Type III, Type IV, or Type V fluid-phase behavior. However, because no binary CO_2 systems are known to show Type V behavior in the literature, and because the occurrence of a Type IV system is rare, the system CO_2 + [bmim][PF_6] most likely has Type III fluid-phase behavior. Table 2 summarizes the LLV data of the system CO_2 + [bmim][PF_6] and the LV data of pure CO_2. Figure 5 graphically compares the LLV data of the system CO_2 + [bmim][PF_6] and the LV data of pure CO_2. The very minor differences between the location of the LLV three-phase locus of the system CO_2 + [bmim][PF_6] and the LV line of pure CO_2 and also the very small difference of the location of the critical endpoint (L_1 = V) + L_2 of the binary system CO_2 + [bmim][PF_6] compared to the critical point of pure CO_2 prove that the solubility of [bmim][PF_6] in CO_2 is extremely low.

The system CHF_3 + [bmim][PF_6]

The second system studied in this work was the binary CHF_3 + [bmim][PF_6]. CHF_3 has a strong permanent dipole moment,

Table 2. The P–T Data of the LLV Boundary of the System CO_2 + [bmim][PF_6] and the LV Data of Pure CO_2

CO_2 + [bmim][PF_6]		Pure CO_2	
T (K)	P (MPa)	T (K)	P (MPa)
293.14	5.73	293.21	5.74
293.16	5.73	295.65	6.09
294.38	5.89	297.19	6.30
295.62	6.07	298.10	6.43
295.73	6.09	299.13	6.59
296.18	6.14	300.16	6.74
296.68	6.22	301.21	6.90
297.16	6.29	302.20	7.06
297.46	6.33	303.16	7.21
297.70	6.36	303.17	7.23
298.14	6.43	303.66	7.30
298.23	6.43	304.11	7.37
299.20	6.59	304.19**	7.39
299.25	6.59		
300.23	6.74		
301.14	6.88		
302.14	7.04		
302.20	7.04		
303.15	7.20		
304.16	7.36		
304.20	7.37		
304.23*	7.38		

*The critical endpoint of the binary system CO_2 + [bmim][PF_6].
**The critical point of pure CO_2.

whereas CO_2 does not have any dipole moment. Therefore, it is expected that the interaction between CHF_3 and [bmim][PF_6] is stronger, resulting in a different behavior of the mixture of CHF_3 and [bmim][PF_6] compared to that of the system CO_2 + [bmim][PF_6].

The phase behavior of the binary system of CHF_3 + [bmim][PF_6] was determined by measuring its LV boundaries for 15 different isopleths. The results of these measurements, presented in Table 3, indicate that the solubility of CHF_3 in [bmim][PF_6] is remarkably high. For instance, at 313.24 K and at a pressure of only 3.75 MPa, the solubility of CHF_3 in [bmim][PF_6] is 0.483 in the mole fraction. Therefore, if experiments show a negligible solubility of [bmim][PF_6] in supercritical CHF_3, similar to that of CO_2, CHF_3 can also be a potentially attractive supercritical solvent for extracting solutes from [bmim][PF_6] with no cross-contamination. By analyzing the data in Table 3, it is evident that the equilibrium pressure increases isothermally with increasing CHF_3 composition up to a certain value (critical pressure), after which there is a decline in the equilibrium pressure with further isothermal increase of the CHF_3 concentration. This can be better explained in the perspective of a P–x diagram.

Because both bubble- and dew-point data are available in Table 3, the isothermal interpolation of these data onto a P–x diagram can provide information on both the solubility of the supercritical fluid in the ionic liquid-rich phase and the solubility of the ionic liquid in the supercritical fluid phase. This is very important information for a process in which a solute is extracted from an ionic liquid using a supercritical fluid.

Figure 6 shows this information in a P–x diagram of the system CHF_3 + [bmim][PF_6] at 335, 340, and 345 K. The maximum in each isotherm indicates the location of the critical point of the system at that particular temperature. This figure shows that the liquid–vapor critical composition of this system does not vary significantly throughout the temperature range investigated. Table 4 summarizes the interpolated critical compositions and pressures for the system CHF_3 + [bmim][PF_6] for several isotherms. It is also seen that the solubility of [bmim][PF_6] in supercritical CHF_3 is significant in the region near the critical point of the system, whereas it sharply decreases by isothermally decreasing the pressure. As expected, the solubility of CHF_3 in the ionic liquid-rich phase decreases with an increase in temperature. Figure 6 also illustrates that the temperature dependency of the CHF_3 solubility in [bmim][PF_6] is not significant at lower CHF_3 concentrations; however, when x_{CHF3} increases, the temperature dependency of the CHF_3 solubility gradually increases until the critical composition of the mixture is reached.

To determine the type of phase behavior of the system CHF_3 + [bmim][PF_6], a mixture of 98.01 mol % of CHF_3 and 1.99 mol % of [bmim][PF_6] was studied in the Cailletet apparatus. The mixture also showed a three-phase LLV equilibrium at pressures and temperatures close to the LV saturated vapor pressure locus of pure CHF_3. This mixture also had a critical endpoint very close to the critical point of pure CHF_3. Figure 7 graphically shows the LLV results of this system. The critical endpoint had the nature of (L_1 = V) + L_2, that is, for the system CHF_3 + [bmim][PF_6] Type III, Type IV, or Type V might hold. Because no lower critical endpoint L_1 + (L_2 = V) could be established in this system, and as previously indicated that Type IV systems are very rare, Type III fluid-phase behavior was also assigned to this system. Table 5 summarizes the LLV data of this system up to its critical endpoint and the

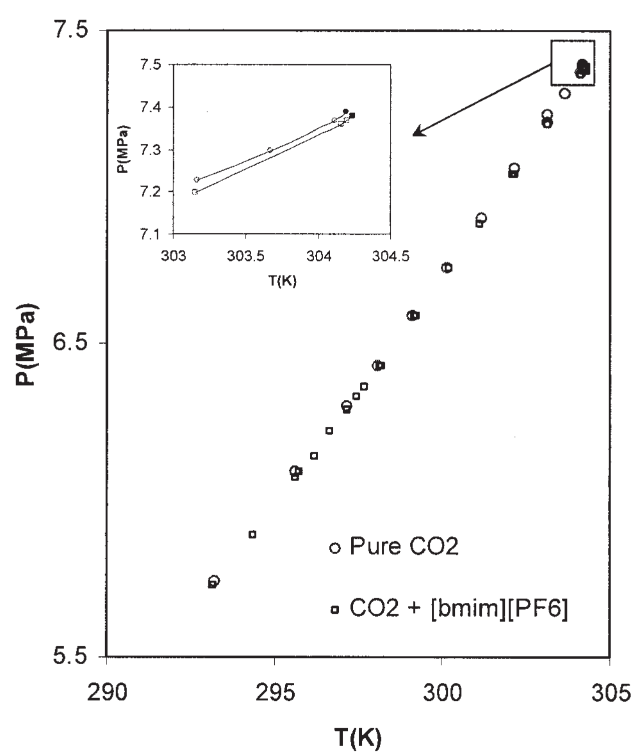

Figure 5. LLV boundary of the system CO_2 + [bmim][PF_6] and the LV boundary of pure CO_2.

"●" indicates the critical point of CO_2 and "■" indicates the (L_1 = V) + L_2 critical endpoint of the system CO_2 + [bmim][PF_6].

Table 3. Vapor–Liquid Equilibrium Data for Various Compositions (in mole fraction) of Trifluoromethane in the CHF_3 + [bmim][PF_6] System

x_{CHF3}*	T (K)	P (MPa)	T (K)	P (MPa)	T (K)	P (MPa)
0.102 (b.p.)	303.20	0.58	328.24	0.88	353.23	1.24
	308.19	0.63	333.22	0.94	358.22	1.33
	313.20	0.69	338.17	1.02	363.25	1.41
	318.18	0.74	343.25	1.09		
	323.26	0.82	348.22	1.17		
0.203 (b.p.)	303.29	1.16	328.22	1.81	353.27	2.62
	308.21	1.28	333.30	1.96	358.23	2.80
	313.25	1.40	338.23	2.11	363.39	2.98
	318.24	1.54	343.29	2.28		
	323.31	1.67	348.26	2.45		
0.302 (b.p.)	303.28	1.78	328.26	2.85	353.32	4.17
	308.30	1.97	333.28	3.08	358.33	4.49
	313.28	2.18	338.29	3.35	363.31	4.79
	318.25	2.38	343.32	3.62		
	323.32	2.61	348.29	3.89		
0.400 (b.p.)	303.38	2.43	328.33	3.97	353.36	5.99
	308.33	2.69	333.39	4.33	358.22	6.43
	313.32	2.97	338.30	4.71	363.15	6.91
	318.24	3.27	343.36	5.13		
	323.33	3.61	348.27	5.55		
0.483 (b.p.)	303.24	3.01	328.33	5.11	353.25	7.99
	308.22	3.37	333.29	5.65	358.30	8.67
	313.24	3.75	338.31	6.19	363.42	9.41
	318.34	4.17	343.32	6.75		
	323.28	4.61	348.25	7.37		
0.552 (b.p.)	313.15	4.56	327.79	6.36	342.66	8.76
	318.09	5.12	332.77	7.14	347.62	9.68
	322.77	5.68	337.73	7.94	352.57	10.60
0.621 (b.p.)	312.75	5.28	332.63	8.92	347.51	12.54
	317.76	6.02	337.65	10.10	352.43	13.80
	322.77	6.88	342.56	11.30	357.26	15.06
	327.70	7.84				
0.700 (b.p.)	312.95	7.84	332.80	14.64	347.43	19.70
	317.84	9.50	337.71	16.36	352.30	21.32
	322.81	11.22	342.62	18.04	357.12	22.88
	327.80	12.92				
0.780 (b.p.)	312.90	14.20	327.88	20.52	342.80	26.44
	317.98	16.30	332.85	22.50	347.69	28.32
	322.93	18.44	337.82	24.48	352.73	30.28
0.850 (b.p.)	313.11	19.44	332.79	27.72	347.53	33.62
	317.86	21.50	337.72	29.64	352.39	35.56
	322.90	23.64	342.58	31.62	357.42	37.54
	327.79	25.68				
0.900 (b.p.)	312.85	20.60	332.80	29.54	347.92	35.98
	318.36	23.12	337.79	31.70	352.56	37.90
	323.73	25.54	342.73	33.82	358.16	40.16
	327.87	27.38				
0.925 (b.p.)	312.95	21.60	332.88	30.52	347.99	36.94
	317.86	23.84	337.83	32.66	352.66	38.86
	322.95	26.14	342.69	34.72	357.50	40.82
	327.79	28.28				
0.956 (d.p.)	312.94	21.76	333.82	31.06	352.67	38.98
	320.01	24.96	340.74	34.02	357.64	41.00
	326.87	28.02	347.69	36.94		
0.980 (d.p.)	313.48	21.62	332.83	30.12	347.68	36.34
	317.90	23.60	337.83	32.26	352.68	38.36
	322.92	25.82	342.69	34.28	357.56	40.30
	327.91	28.00				
0.990 (d.p.)	312.86	19.48	328.30	26.00	343.48	32.08
	317.93	21.66	332.84	27.82	348.15	33.94
	322.89	23.74	338.66	30.18	352.78	35.74

*b.p. indicates bubble point measurements; d.p. indicates dew point measurements.

LV data of pure CHF_3 up to its critical point as well. Because the difference between the critical endpoint of the system CHF_3 + [bmim][PF_6] and the critical point of CHF_3 is greater than the difference between the corresponding points in the CO_2 + [bmim][PF_6] system, it can be concluded that [bmim][PF_6] is more soluble in the CHF_3 phase, having greater effects on the $L_1 = V$ behavior.

Figure 8a shows the P–T projection of the system CHF_3 +

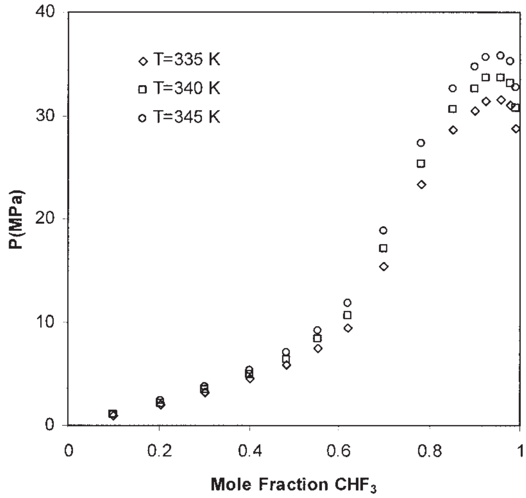

Figure 6. ***P–x* diagrams of the system CHF_3 + [bmim][PF_6] at 335, 340, and 345 K.**

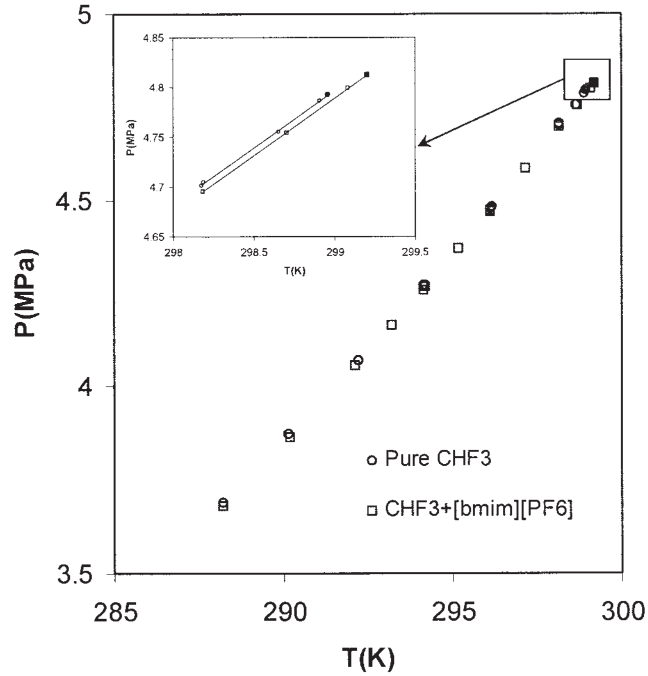

Figure 7. LLV boundary of the system CHF_3 + [bmim][PF_6] and the LV boundary of pure CHF_3.

"●" indicates the critical point of CHF_3 and "■" indicates the (L_1 = V) + L_2 critical endpoint of the system CHF_3 + [bmim][PF6].

[bmim][PF_6], obtained from the experiments in this study. It shows that the critical locus of this system has a positive slope. This critical line is located between the critical temperatures of CHF_3 and that of the IL. Therefore, we can expect the complete critical loci of the system CHF_3 + [bmim][PF_6] to have the shape of either branch 1 or branch 2 in Figure 8b.

Figure 9 shows the differences between the phase behavior of the systems CHF_3 + [bmim][PF_6] and CO_2 + [bmim][PF_6] at 340 K. First of all, the solubility of CHF_3 in [bmim][PF_6] is greater than the solubility of CO_2 in [bmim][PF_6]. It is also obvious from Figure 9 that the critical locus of the system with CO_2 may be located at much higher pressures. The binary system with CHF_3 shows a closed phase envelope, including the occurrence of a critical point, whereas the CO_2 binary system has an immiscibility gap between the supercritical phase and the IL-rich phase, even up to very high pressures. This can be attributable to stronger molecular interactions between CHF_3 and [bmim][PF_6] compared to those between CO_2 and [bmim][PF_6]. CHF_3 has a permanent dipole moment (=1.65 Debye), whereas CO_2 has no dipole moment. As discussed extensively by Levelt Sengers,[36] binary mixtures of a strongly interacting solvent and a volatile component can have critical lines that run to much lower temperatures and pressures than is the case in binary systems of the same solvent with a less interacting volatile molecule. Therefore, the critical locus of the system CO_2 + [bmim][PF_6] is expected to have the shape of either branch 3 or branch 4 in Figure 8b.

Table 4. Interpolated Critical Pressures and Compositions of the System CHF_3 + [bmim][PF_6] for Some Isotherms

T (K)	*P* (MPa)	x_{CHF3}
315	22.77	0.9486
320	25.04	0.9479
325	27.27	0.9473
330	29.48	0.9467
335	31.65	0.9462
340	33.79	0.9456
345	35.90	0.9452
350	37.97	0.9447
355	40.02	0.9443

Recently, Shariati and Peters[33] reported the phase behavior of the system CHF_3 + [emim][PF_6]. Figure 10 compares the isothermal phase behavior of the systems CHF_3 + [bmim][PF_6] and CHF_3 + [emim][PF_6] at 345 K. It is seen that the solubility of CHF_3 in [bmim][PF_6] is greater than that in [emim][PF_6]. Also, the solubility of [bmim][PF_6] is greater than that of [emim][PF_6] in supercritical CHF_3. This shows how the alkyl chain length of the IL affects the interactions between the IL and the supercritical fluid.

Table 5. *P–T* Data of the LLV Boundary of the System CHF_3 + [bmim][PF_6] and the LV Data of Pure CHF_3

CHF_3 + [bmim][PF_6]		Pure CHF_3	
T (K)	*P* (MPa)	*T* (K)	*P* (MPa)
288.22	3.68	288.24	3.69
290.20	3.86	290.16	3.87
292.14	4.05	292.21	4.07
293.21	4.16	294.19	4.27
294.15	4.26	294.16	4.27
294.20	4.26	296.12	4.47
295.18	4.37	296.18	4.48
296.13	4.47	298.17	4.70
296.16	4.47	198.19	4.71
297.20	4.58	298.65	4.76
298.18	4.69	298.91	4.79
298.70	4.75	298.96**	4.79
299.08	4.80		
299.20*	4.81		

*The critical endpoint of the binary system CHF_3 + [bmim][PF_6].
**The critical point of pure CHF_3.

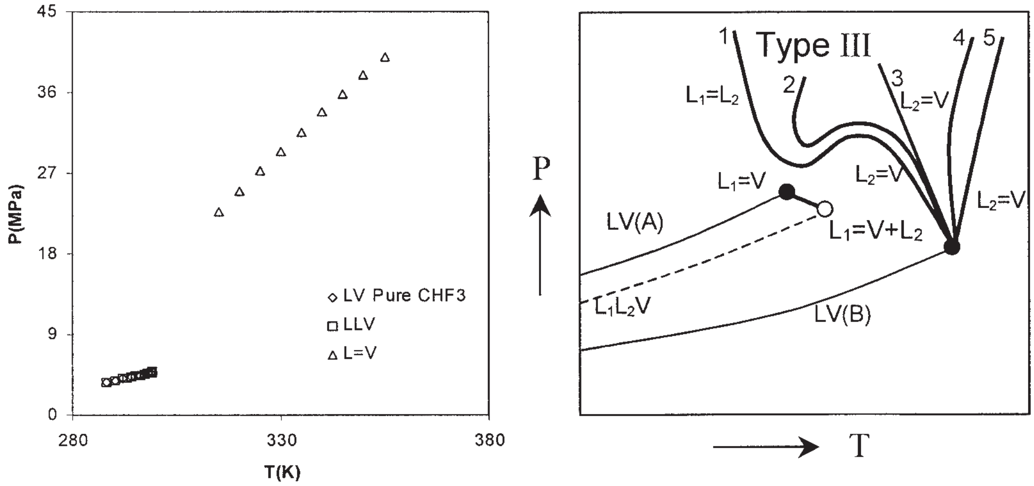

(a) **(b)**

Figure 8. (a) *P–T* projection of the system CHF_3 + [bmim][PF6]; (b) Type III of the fluid-phase behavior classification of Scott and Van Konynenburg.[27]

Conclusions and Summary

In this work, the phase behavior of the binary mixtures of the supercritical fluids CO_2 and CHF_3 and an IL ([bmim][PF_6]) was studied experimentally. Although other researchers had also studied the system CO_2 + [bmim][PF_6],[28-32] this is the first time that its phase behavior has been studied up to highly elevated pressures, its three-phase equilibrium LLV reported, and the type of its phase behavior determined. This study shows that CO_2 has an excellent solubility in [bmim][PF_6] at lower pressures but, instead of having a critical point at moderate pressures, its two-phase boundary extends almost vertically up to very high pressures. According to our study, Type III fluid-phase behavior can be assigned to the system CO_2 + [bmim][PF_6]. We have also shown the similarities in phase behavior of binary systems of CO_2 and three members of the 1-alkyl-3-methylimidazolium hexafluorophosphate homologous family. The effect on the solubility of CO_2 in each of the three ILs belonging to the same homologous family, as a function of the alkyl chain length of the three ILs, has also been determined. For the systems investigated, a linear relationship between the alkyl chain length and the solubility of CO_2 in the three ILs was established.

The phase behavior of the system CHF_3 + [bmim][PF_6] has been studied for the first time in this work. Similar to the system CO_2 + [bmim][PF_6], this binary system most likely also shows Type III fluid-phase behavior. However, CHF_3 shows stronger interaction than CO_2 with the IL. For this reason, the critical locus of the system CHF_3 + [bmim][PF_6] is

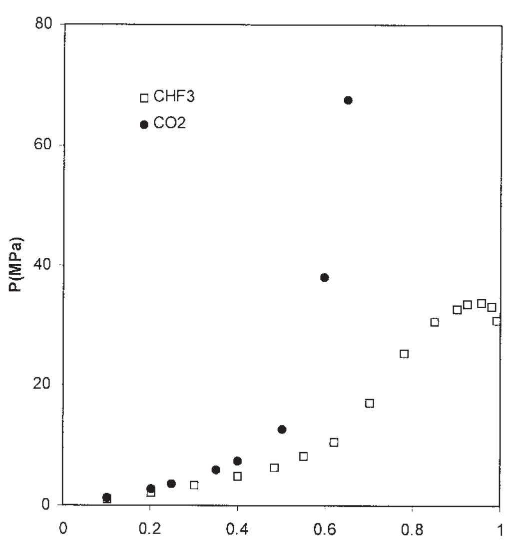

Figure 9. Comparison between the phase behavior of the systems CHF_3 + [bmim][PF_6] and CO_2 + [bmim][PF_6] at 340 K.

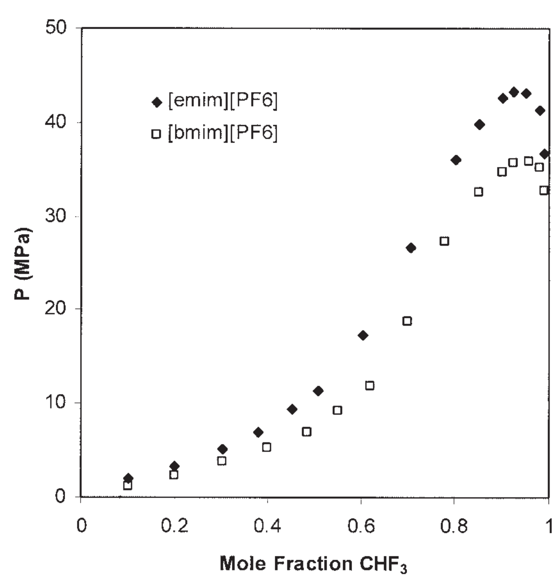

Figure 10. Comparison between the phase behavior of the systems CHF_3 + [bmim][PF_6] and CHF_3 + [emim][PF_6] at 345 K.

located at lower pressures and lower temperatures as well, enabling us to measure the solubility of the IL in the supercritical phase. Furthermore, it was shown that the phase behavior of the systems CHF_3 + [emim][PF_6] and CHF_3 + [bmim][PF_6] are similar. However, CHF_3 has a better solubility in [bmim][PF_6] than that in [emim][PF_6].

Acknowledgments

The authors sincerely thank Prof. Seddon of the Queen's University of Belfast, Northern Ireland for kindly providing the ionic liquid required for the CHF_3 + [bmim][PF_6] measurements.

Literature Cited

1. Seddon KR, Stark A, Torres MJ. Influence of chloride, water, and organic solvents on the physical properties of ionic liquids. *Pure Appl Chem*. 2000;72:2275-2287.
2. Aki SNVK, Brennecke JF, Samanta A. How polar are room-temperature ionic liquids? *Chem Commun*. 2001;5:413-414.
3. Brennecke JF, Maginn EJ. Ionic liquids: Innovative fluids for chemical processing. *AIChE J*. 2001;47:2384-2389.
4. Bao W, Wang Z, Li Y. Synthesis of chiral ionic liquids from natural amino acids. *J Org Chem*. 2003;68:591-593.
5. Holbrey JD, Reichert WM, Swatloski RP, Broker GA, Pitner WR, Seddon KR, Rogers RD. Efficient, halide free synthesis of new, low cost ionic liquids: 1,3-Dialkylimidazolium salts containing methyl- and ethyl-sulfate anions. *Green Chem*. 2002;4:407-413.
6. Mirzaei YR, Twamley B, Shreeve JM. Synthesis of 1-alkyl-1,2,4-triazoles and the formation of quaternary 1-alkyl-4-polyfluoroalkyl-1,2,4-triazolium salts leading to ionic liquids. *J Org Chem*. 2002;67:9340-9345.
7. Singh RP, Manandhar S, Shreeve JM. New dense fluoroalkyl-substituted imidazolium ionic liquids. *Tetrahedron Lett*. 2002;43:9497-9499.
8. Forsyth S, Golding J, MacFarlane DR, Forsyth M. *N*-Methyl-*n*-alkylpyrrolidinium tetrafluoroborate salts: Ionic solvents and solid electrolytes. *Electrochim Acta*. 2001;46:1753-1757.
9. Wilkes JS, Zaworotko MJ. Air and water stable 1-ethyl-3-methylimidazolium based ionic liquids. *J Chem Soc Chem Commun*. 1992;13:965-967.
10. Lagrost C, Carrie D, Vaultier M, Hapiot P. Reactivities of some electrogenerated organic cation radicals in room temperature ionic liquids: Toward an alternative to volatile organic solvents? *J Phys Chem A*. 2003;107:745-752.
11. Olivier-Bourbigou H, Magna L. Ionic liquids: Perspectives for organic and catalytic reactions. *J Mol Catal A Chem*. 2002;182-183:419-437.
12. Seddon KR, Stark A. Selective catalytic oxidation of benzyl alcohol and alkylbenzenes in ionic liquids. *Green Chem*. 2002;4:119-123.
13. Buijsman RC, van Vuuren E, Sterrenburg JG. Ruthenium-catalyzed olefin metathesis in ionic liquids. *Org Lett*. 2001;3:3785-3787.
14. Gordon CM. New developments in catalysis using ionic liquids. *Appl Catal A Gen*. 2001;222:101-117.
15. Earle MJ, McCormac PB, Seddon KR. The first high yield green route to a pharmaceutical in a room temperature ionic liquid. *Green Chem*. 2000;2:261-262.
16. Welton T. Room-temperature ionic liquids. Solvents for synthesis and catalysis. *Chem Rev*. 1999;99:2071-2083.
17. Adams CJ, Earle MJ, Roberts G, Seddon KR. Friedel–Crafts reactions in room temperature ionic liquids. *Chem Commun*. 1998;19:2097-2098.
18. Abraham MH, Zissimos AM, Huddleston JG, Willauer HD, Rogers RD, Acree WE. Some novel liquid partitioning systems: Water-ionic liquids and aqueous biphasic systems. *Ind Eng Chem Res*. 2003;42:413-418.
19. Najdanovic-Visak V, Esperanca JMSS, Rebelo LPN, Nunes da Ponte M, Guedes HJR, Seddon KR, Szydlowski J. Phase behaviour of room temperature ionic liquid solutions: An unusually large co-solvent effect in (water + ethanol). *Phys Chem Chem Phys*. 2002;4:1701-1703.
20. Swatloski RP, Visser AE, Reichert WM, Broker GA, Farina LM, Holbrey JD, Rogers RD. On the solubilization of water with ethanol in hydrophobic hexafluorophosphate ionic liquids. *Green Chem*. 2002;4:81-87.
21. Wong DSH, Chen JP, Chang JM, Chou CH. Phase equilibria of water and ionic liquids [emim][PF_6] and [bmim][PF_6]. *Fluid Phase Equilib*. 2002;194-197:1089-1095.
22. Anthony JL, Maginn EJ, Brennecke JF. Solution thermodynamics of imidazolium-based ionic liquids and water. *J Phys Chem B*. 2001;105:10942-10949.
23. Huddleston JG, Willauer HD, Swatloski RP, Visser AE, Rogers RD. Room temperature ionic liquids as novel media for "clean " liquid–liquid extraction. *Chem Commun*. 1998;16:1765-1766.
24. Blanchard LA, Brennecke JF. Recovery of organic products from ionic liquids using supercritical carbon dioxide. *Ind Eng Chem Res*. 2001;40:287-292.
25. Scurto AM, Aki SNVK, Brennecke JF. CO_2 as a separation switch for ionic liquid/organic mixtures. *J Am Chem Soc*. 2002;124:10276-10277.
26. Scurto AM, Aki SNVK, Brennecke JF. Carbon dioxide induced separation of ionic liquids and water. *Chem Commun*. 2003;5:572-573.
27. Scott RL, Van Konynenburg PH. Van der Waals and related models for hydrocarbon mixtures. *Discuss Faraday Soc*. 1970;49:87-97.
28. Blanchard LA, Hancu D, Beckman EJ, Brennecke JF. Green processing using ionic liquids and CO_2. *Nature*. 1999;399:28-29.
29. Blanchard LA, Gu Z, Brennecke JF. High-pressure phase behavior of ionic liquid/CO_2 systems. *J Phys Chem B*. 2001;105:2437-2444.
30. Anthony JL, Maginn EJ, Brennecke JF. Solubilities and thermodynamic properties of gases in the ionic liquid 1-*n*-butyl-3-methylimidazolium hexafluorophosphate. *J Phys Chem B*. 2002;106:7315-7320.
31. Perez-Salado Kamps A, Tuma D, Xia J, Maurer G. Solubility of CO_2 in the ionic liquid [bmim][PF_6]. *J Chem Eng Data*. 2003;48:746-749.
32. Liu Z, Wu W, Han B, Dong Z, Zhao G, Wang J, Jiang T, Yang G. Study on the phase behaviors, viscosities, and thermodynamic properties of CO_2/[C_4mim][PF_6]/methanol system at elevated pressures. *Chem Eur J*. 2003;9:3897-3903.
33. Shariati A, Peters CJ. High-pressure phase behavior of systems with ionic liquids: I. Measurements and modeling of the binary system fluoroform + 1-ethyl-3-methylimidazolium hexafluorophosphate. *J Supercrit Fluids*. 2003;25:109-117.
34. Shariati A, Peters CJ. High-pressure phase behavior of systems with ionic liquids: II. The binary system carbon dioxide + 1-ethyl-3-methylimidazolium hexafluorophosphate. *J Supercrit Fluids*. 2004;29:43-48.
35. Shariati A, Peters CJ. High-pressure phase behavior of systems with ionic liquids: III. The binary system carbon dioxide + 1-hexyl-3-methylimidazolium hexafluorophosphate. *J Supercrit Fluids*. 2004;30:139-144.
36. Levelt Sengers JMH. Solubility near the solvent's critical point. *J Supercrit Fluids*. 1991;4:215-222.

Manuscript received Apr. 29, 2004, and revision received Aug. 23, 2004.